

## DRAG ON NON-SPHERICAL PARTICLES IN NON-NEWTONIAN FLUIDS

Hassan A. Farag\* and \*\*Nawaf H. El-Manaa

\*Professor, Department of Chemical Engineering, University of Qatar  
Doha, Qatar.

\*\* Department of Standards and Measurements, Ministry of Finance  
Doha, Qatar.

### ABSTRACT

The drag coefficient ( $C_D$ ) was determined for three different non-spherical particles (cubes, rectangles and cylinders) of different sizes falling in two different non-Newtonian fluids (glycerol and polymer - paraffin oil mixture) using the terminal velocity technique. The variation of the drag coefficient with the variation of non-spherical particle size was explained. Also the relation between  $C_D$  and  $Re_0$  (0.25-5) is graphically compared with those previously published in the literature for discs and cylinders with infinite length. Moreover some mathematical relations, previously published in the literature, are verified for the three tested non-spherical particles.

### NOMENCLATURE

$A_p$	:	Projected area of particle in a plane perpendicular to direction of motion, $m^2$
$C_D$	:	Drag coefficient
$d_p$	:	Particle diameter, m
$D_s$	:	Spherical diameter = diameter of a sphere whose volume is equal to the volume of the tested particle, m
$F_b$	:	Bouancy force on the particle, N
$F_d$	:	Drag force, N
$F_g$	:	Gravity force on the particle, N
$g$	:	Acceleration of gravit, $m/s^2$
$g_c$	:	Newton's Law proportionality factor
$K'$	:	A constant used for calculating the volume of non-spherical particles; its value depends on particle shape
$m$	:	Mass of particle, kg

- $R_o'$  : Force per unit of projected area of particle on a plane perpendicular to the direction of motion (at terminal falling velocity),  $N/m^2$   
 $Re_o$  : Modified Reynolds number (at terminal falling velocity)  
 $u$  : Particle velocity in the fluid, m/s  
 $u_o$  : Terminal falling velocity of the particle, m/s  
 $u_{ot}$  : Terminal falling velocity of the particle in a tube, m/s  
 $t$  : Time of particle motion in the fluid, sec.  
 $\psi$  : Sphericity of the non-spherical particle = surface area of a sphere having the same volume as the non-spherical particle/surface area of the non-spherical particle,  $m^2$   
 $\rho$  : Fluid density,  $kg/m^3$   
 $\rho_p$  : Particle density,  $kg/m^3$

## INTRODUCTION

Data on the resisting forces acting on bodies moving through fluids are invaluable in the design and operation of equipment where controlled particle motion is of importance, such as in the case of crystallization, classification, centrifugation and dust-collection equipment.

The study of drag coefficients for a number of geometrical configurations has been presented in the literature as early as 1851 (3). Because of their geometrical simplicity, spheres have been thoroughly investigated both from theoretical and experimental considerations (1,2,3).

Pettyjohn and Christiansen (1) gave a good review of early works carried out to study the settling behavior of specified, well-defined, non-spherical particle shapes which are normally encountered in industry. Pettyjohn and Christiansen have determined resistance coefficients for a group of non-Spherical particles of a sphericity range of 0.67 to 0.906 settling in fluids having a viscosity range of 0.0877 to  $9.16 \times 10^4$  cP, using the terminal falling velocity technique. This technique implies that the particle while falling in the fluid will eventually attain a constant velocity, called the terminal falling velocity. At this velocity, the gravity force acting on the particle will be equal to the sum of both bouancy and drag forces acting upwards on the particle. They have covered a range of Reynolds Number from 0.007 to 17,410 for non-spherical particles. They have concluded that sphericity is a satisfactory criterion of the effect of particle shape on the resistance to motion experienced by isometric

particles (particles with equal dimensions around the same axis) moving in a fluid.

Christiansen and Barker (2) have determined drag coefficients using the terminal velocity technique for cylinders, prisms and disks at Reynolds number from  $10^3$  to  $3 \times 10^5$  (in water and air).

Isaacs and Thodos (3) have determined the friction factor  $f_p$  (based on particle projected area) for cylindrical particles, with an aspect ratio (L/D) ranging from 10 to 0.1, and Reynolds number from 200 to  $6 \times 10^4$ . They have found that  $f_p$  was independent of the value of Reynolds number in this range.

Saito et al (4) have studied the free settling behavior of cylindrical particles with an aspect ratio (L/D) ranging from 2 to 3.5 at Reynolds number from 150 to 1000. They have obtained a graphical relation between the drag coefficient and Reynolds number which was parallel to that of spherical particles. For the range of Reynolds number studied the drag coefficient for the cylindrical particles was always higher than that for spherical particles.

It seems that data about the drag coefficients for non-spherical particles (cylinders, cubes and rectangles) in the Reynolds number range 0.1-10 (higher than Stokes law application range) are lacking. The aim of this work is to try to obtain these data for the afore-mentioned non-spherical particles. Also the effect of particle aspect ratio (L/D for cylinders and W/L for rectangles) on the drag coefficients for two different non-Newtonian fluids (glycerol 100% concentrated and paraffin oil polymer mixture) was studied.

## THEORETICAL FORMULATION

### Governing Equations

The drag coefficient is defined by the following equation (5)

$$C_D = \frac{F_d / A_p}{\rho u_o^2 / 2 g_c} \quad (1)$$

where  $F_d$  is total drag force  
 $A_p$  projected area of particle in a plane perpendicular to direction of motion  
 $u_o$  terminal falling velocity of particle

$\rho$  fluid density

$g_c$  Newton's law proportionality factor

It can be calculated by using two equations suggested by McCabe et al., 1985.

**First Method:**

A particle falling in a fluid will be subjected to three forces:  $F_g$  - gravity force;  $F_d$  - drag force (upwards) and  $F_b$  - bouancy force (upwards). Therefore the resultant force ( $F$ ) acting on the particle while falling will be :

$$\begin{aligned} F &= m(du/dt)/g_c = F_g - (F_b + F_d) \\ &= mg/g_c - ( m\rho g/(\rho_p g_c) + C_D u^2 \rho A_p / (2g_c) ) \end{aligned} \quad (2)$$

Dividing by ( $m/g_c$ ):

$$\begin{aligned} \therefore du/dt &= g - (\rho g/\rho_p + C_D u^2 \rho A_p / (2m) ) \\ &= g (\rho_p - \rho) / \rho_p - C_D u^2 \rho A_p / (2m) \end{aligned} \quad (3)$$

At terminal falling velocity there will be zero acceleration, i.e  $du/dt = 0$

$$\therefore C_D = 2 mg (\rho_p - \rho) / (u_0^2 \rho_p A_p \rho) \quad (4)$$

**Second method:**

At terminal falling velocity , for a non-spherical particle, the drag force can be given by :

$$F_d = R_o' (\pi/4) d_p^2 = K'd_p^3 (\rho_p - \rho)g \quad (5)$$

$$\therefore R_o' / (\rho u_o^2) = 4 K'd_p g (\rho_p - \rho) / (\pi \rho u_o^2) \quad (6)$$

$R_o' / (\rho u_o^2)$  is a form of the drag coefficient and may be denoted by  $C_D'$ . Frequently the drag coefficient  $C_D$  is defined as the ratio  $R_o' / (\rho u_o^2 / 2)$

$$\therefore C_D = 2 C_D' = 2R_o' / (\rho u_o^2) = 8K'd_p g (\rho_p - \rho) / (\pi \rho u_o^2) \quad (7)$$

In this work the first method was used to calculate the drag coefficient.

The influence of walls on the terminal falling velocity of the particle can be accounted for by using equation 8.

$$\frac{u_{ot}}{u_o} = \left(1 + 24 \frac{d_p}{d_t}\right)^{-1} \quad \text{for} \quad \frac{d_p}{d_t} < 0.1 \quad (8)$$

where  $u_{ot}$  is the terminal falling velocity of the particle in a tube  
 $u_o$  is the terminal falling velocity of the particle in an infinite  
 expanse of fluid, and  
 $d_t$  tube diameter

## EXPERIMENTAL STUDY

### Test Fluids

Pure glycerol (100% concentrated) and a mixture of light paraffin oil added to an oil treatment polymer (Trade name STP-Oil treatment, distributed by STP Division of first brands Corporation, Danbury, CT, USA) were used. Both fluids were found to be non-Newtonian by testing with Brookfield viscometer (model LVT, spindles No. 1 and 2). Both fluids viscosity increased with increasing rpm (shear rate). For rpm range 1.5 - 30, glycerol gave viscosity point values of 800-975 cP, while paraffin oil - polymer mixture gave viscosity point values of 80-102 cP. Density of glycerol was  $1260 \text{ kg/m}^3$  and for paraffin oil - STP mixture  $960 \text{ kg/m}^3$ .

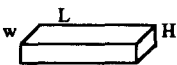
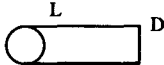
### Test Particles

Particles of different geometrical configurations and dimensions, made of plastic and aluminum ( $\rho = 1274.5$  and  $2651.8 \text{ kg/m}^3$ , respectively) were used. The data of these particles are summarized in table 1. Aluminum particles were used with glycerol, while plastic particles were used for STP-Oil mixture.

### Set-up

A long column made of perspex (inside diameter = 15 cm and height = 164 cm) was used for settling studies. Four equal distances, each of 30 cm, were marked on the column leaving a distance of 25 cm from column bottom to avoid end effect on the falling velocity of the particle. The column had a cover on its top to minimize contact of test fluid surface with air and hence minimize its contamination.

Table 1. Summary of Particles Data

Shape	Characteristic Dimensions, mm
Cube	Side length : 5 - 15
Rectangular	W: 5-15, L:15 , H:3 
Cylinder	D=5 , L=5 - 15 

## Procedure

Single particle is placed on the fluid surface at the center of the column (glycerol or paraffin oil - polymer mixture) and left to start falling from zero velocity. This is the usual technique applied to attain the terminal falling velocity in a short period. Two stop watches (assigned to two research assistants) were used to measure the time required by the particle to cover the last two distances from column bottom. The recorded times were only considered when the difference between them did not exceed 1% to ensure that the particle has attained its terminal falling velocity during the run. Each run was repeated at least three times for each particle.

## RESULTS AND DISCUSSIONS

Figure 1 shows the effect of increasing the size of the cube, expressed as  $L_i/L_1$ , where  $L_i$  is side dimension of any cube and  $L_1 = 5$  mm, on drag coefficient of cubes while falling in the two test fluids. All cubes fell with their sides vertical, i.e. parallel to the direction motion. It is clear from this figure that increasing cube size decreases drastically (almost to 1/16 of its value for the smallest cube) the drag coefficient in the case of glycerol. On the other hand, for STP-Oil mixture, there is a slight decrease in the value of drag coefficient as the cube size increases.

This drastic decrease of drag coefficient in case of glycerol may be attributed to the increase of  $u_o$  and  $m$ . On examining equation 4 which was used to calculate drag coefficient it becomes obvious that although both  $m$  and  $u_o$  increase with the increase in cube size, yet the change in the value of drag coefficient will be more sensitive to the change in the value of  $u_o$ . In case of

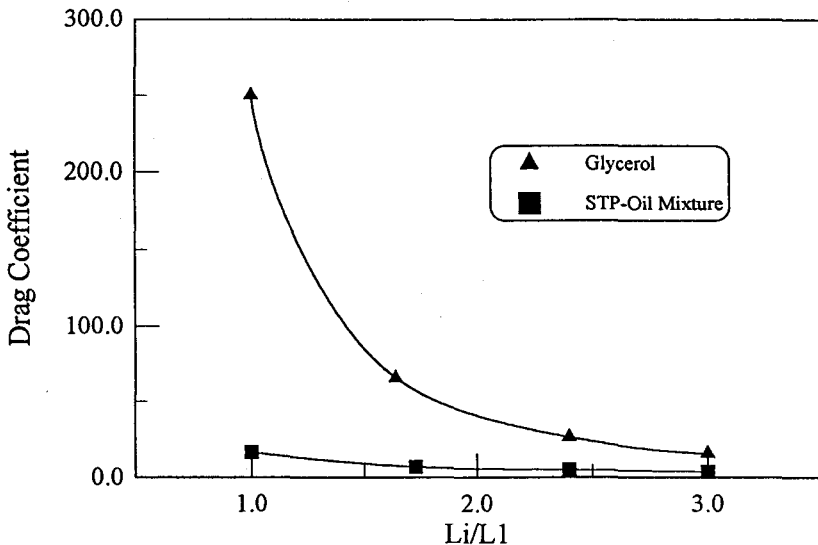


Fig. 1. Drag coefficient vs. size ratio for cubic particles

STP-Oil mixture it seems that the increase in cube mass is slightly counter balanced by the increase in  $u_o$  and  $A_p$

Again for glycerol the increase in the value of  $u_o$  is much higher than that for cube mass. Actually on checking by calculation it was found that increasing cube side almost 3 times led to the increase in its mass almost 27 times, but the increase in  $u_o^2$  was almost 50 times (refer to table 2). For STP-Oil mixture the corresponding increase in  $u_o^2$  was only 9 times. While falling cubic particles had their sides parallel to the direction of motion.

Figure 2 shows the effect of changing width/length (W/L) of rectangular particles on the drag coefficient on falling in glycerol and STP-Oil mixture. While falling the rectangular particles had their largest flat area (face = W.L) perpendicular to the direction of motion. As with cubes, in case of glycerol, increasing W/L (and hence mass and volume of the particle) leads to a marked decrease (almost to 1/3 of its original value at W/L = 0.347) in the value of drag coefficient. In case of STP-Oil mixture, there is slight decrease in the value of the drag coefficient. Referring to equation 4 and table 2, the same reasoning applied for the case of cubes can be used to explain the effect of increasing the dimensions ratio (W/L) on the value of the drag coefficient in case

Table 2. Limit Values of Drag Coefficient and the Corresponding Increase in Particles Mass,  $u_o^2$  and Projected Area ( $A_p$ )

Fluid	Particle	Dimension Ratio	$C_D$	Percent Increase in		
				Mass	$A_p$	$u_o^2$
GLYCEROL	Cube	$L_i/L_1 = 1.0$	250.04	---	---	---
		$L_i/L_1 = 2.97$	15.43	2680	888	930
	Rectangular	$W/L = 0.374$ $W/L = 1.02$	110.20 36.04	---	---	---
	Cylinder	$L/D = 1.2$ $L/D = 3.06$	184.52 89.92	---	---	---
STP-OIL MIXTURE	Cube	$L_i/L_1 = 1.0$	16.32	---	---	---
		$L_i/L_1 = 3.0$	3.78	2690	1743	900
	Rectangular	$W/L = 0.303$ $W/L = 1.047$	16.75 6.33	---	---	---
	Cylinder	$L/D = 1.1$ $L/D = 3.0$	20.16 10.85	---	---	---

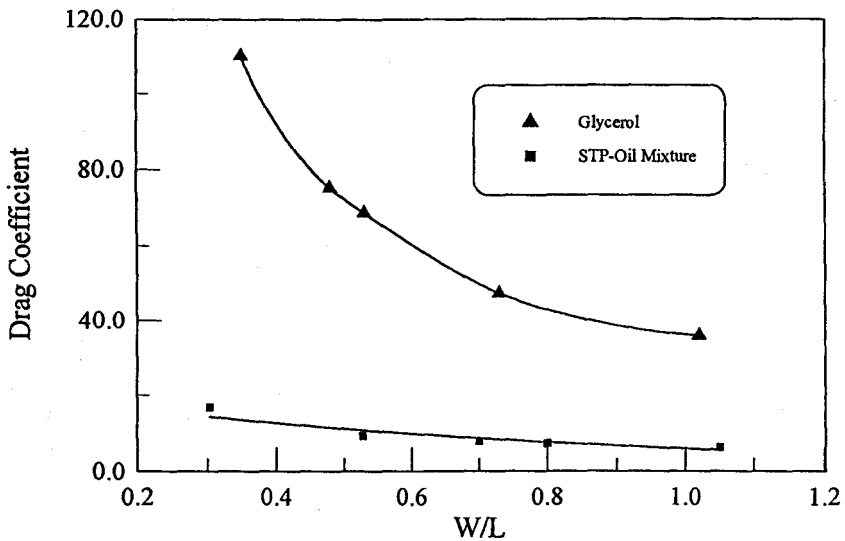


Fig. 2. Drag coefficient vs. size ratio for rectangular particles



of glycerol. Rectangular particles, while falling, had their largest flat area (face) perpendicular to the direction of motion.

Figure 3 shows the effect of changing the aspect ratio ( $L/D$ ) of cylindrical particles on the drag coefficient. The cylinders were oriented while falling with their axis perpendicular to the direction of motion. Again, as with cubes and

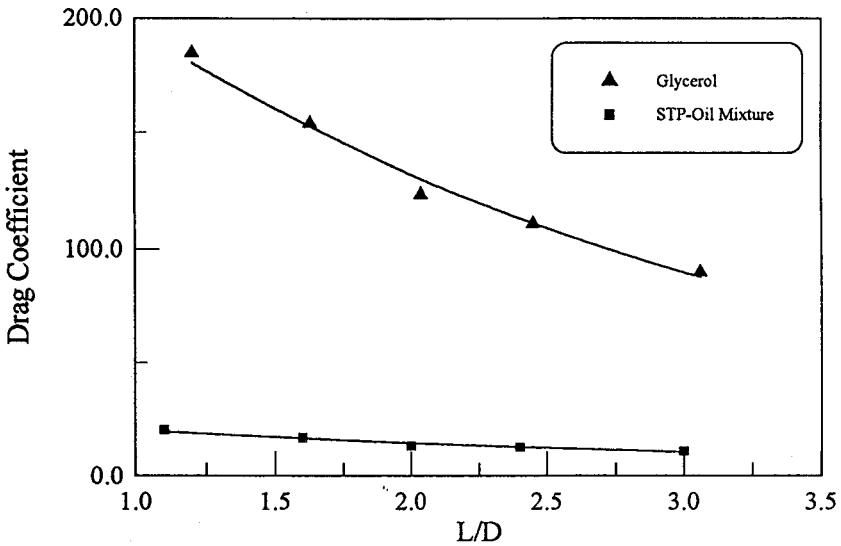
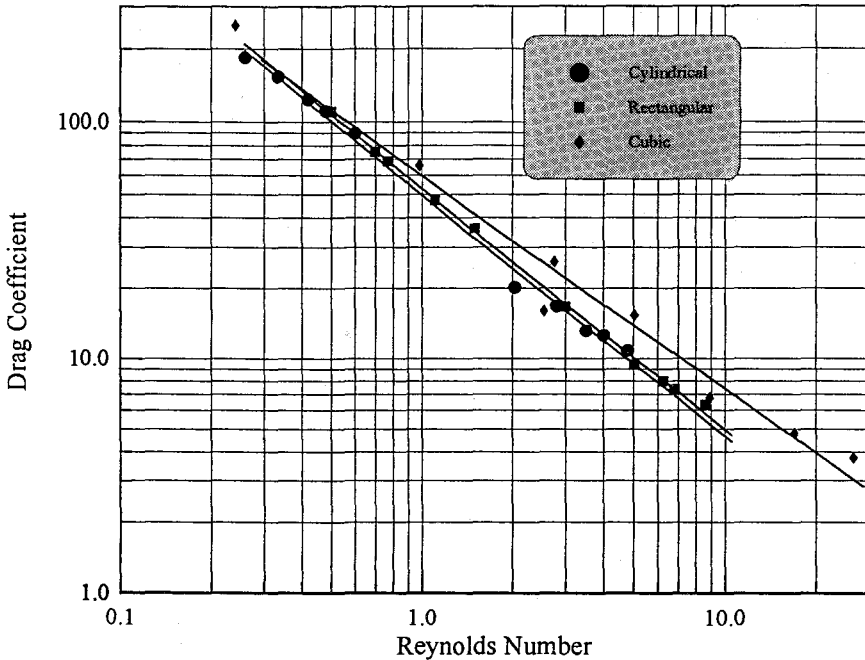


Fig. 3. Drag coefficient vs. size ratio for cylindrical particles

rectangular particles, in case of glycerol, increasing the aspect ratio (and hence mass and volume) leads to a marked decrease (almost to  $\frac{1}{2}$  of its value at  $L/D = 1.2$ ) in the value of drag coefficient. In case of STP-Oil mixture there is slight decrease in the drag coefficient. The same reasoning mentioned for figure 1 can also be applied here. Nevertheless on examining figures 1 and 3 it becomes clear that size increase for cubes has a more pronounced effect on the value of drag coefficient, as compared to size increase for cylindrical particles.

Figure 4 shows the variation of drag coefficient of the tested non-spherical particles and modified Reynolds number ( $d_p u_o \rho / \mu$ ) plotted on a log - log scale (as is usually reported in the literature). For all the tested non-spherical particles increasing Reynolds number decreases the drag coefficient (for both tested fluids, for a Reynolds number range 0.25 - 27). This decrease can be explained as follows:



**Fig. 4. Drag coefficient for tested non-spherical particles**

Increasing the modified Reynolds number for the particles with one fluid means increasing  $d_p$  or  $u_o$  or both. Increasing  $d_p$  means increasing particle mass and hence its terminal falling velocity ( $u_o$ ) increases. From equation 4 it can be seen that variation of  $u_o$  has a greater affect on the value of  $C_D$  than the variation of  $m$ .

Figure 5 shows the comparison of the obtained  $C_D \cdot N_{RE}$  relation for the tested cylindrical particles with those for spherical and cylindrical particle with infinite length, previously published in the literature (7). As expected, cylindrical particles gave higher values of  $C_D$  as compared to those for spheres at the same value of modified Reynolds number. Here it is again emphasized that the tested cylindrical particles were falling with their axes perpendicular to the direction of motion. In this case we can expect that spheres will face less resistance to its motion (expressed as the drag coefficient) while falling in the test fluid. But higher values of  $C_D$  for the tested cylindrical particles as compared to cylindrical particles with infinite length can be explained as follows:

If we use cylinders of both types (with finite and infinite lengths) of equal volumes (of the same material) so that  $u_o$  will be equal; the value of  $d_p$  for the

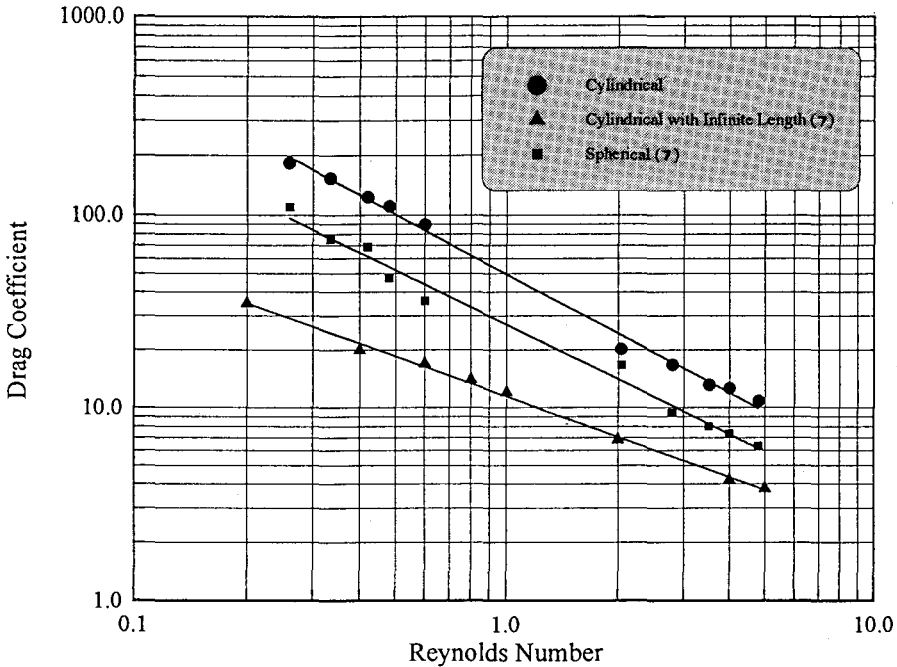


Fig. 5. Drag coefficient for cylinder, cylinder of infinite length and spheres

cylinder with infinite length will be much smaller than that for cylinders with finite length. Consequently the value of modified Reynolds number will be much smaller. In order to have the same value of modified Reynolds number for both particles, we have to increase both  $d_p$  and  $u_o$  for cylinder with infinite length. Increasing  $d_p$  for cylinders with infinite length leads to the increase of  $m$ ,  $u_o$  and  $A_p$ . The net result is the decrease of  $C_D$  (refer to equation 4).

Figures 6, 7 and 8 show the plot of  $R'_o / \rho u_o^2$  vs  $Re_o^{-1}$  for the three tested non-spherical particles: cubic, rectangular and cylindrical, respectively.  $Re_o$  is the modified Reynolds number using  $u_o$  (terminal falling velocity). From these figures the equations shown in table 3 has been obtained. These equations are similar to those published (6) for spherical particles in the same range of Reynolds number (0.2-500). As expected the coefficient of  $Re_o^{-1}$  in case of non-spherical particles (25.1 - 30.15) is much higher than that for spherical particles (6). This means that at the same value of Reynolds number, non-spherical particles will face more drag while falling in the test fluids, as compared to spheres, since  $R'_o / \rho u_o^2 = \frac{1}{2} C_D$  (refer to equation 7).

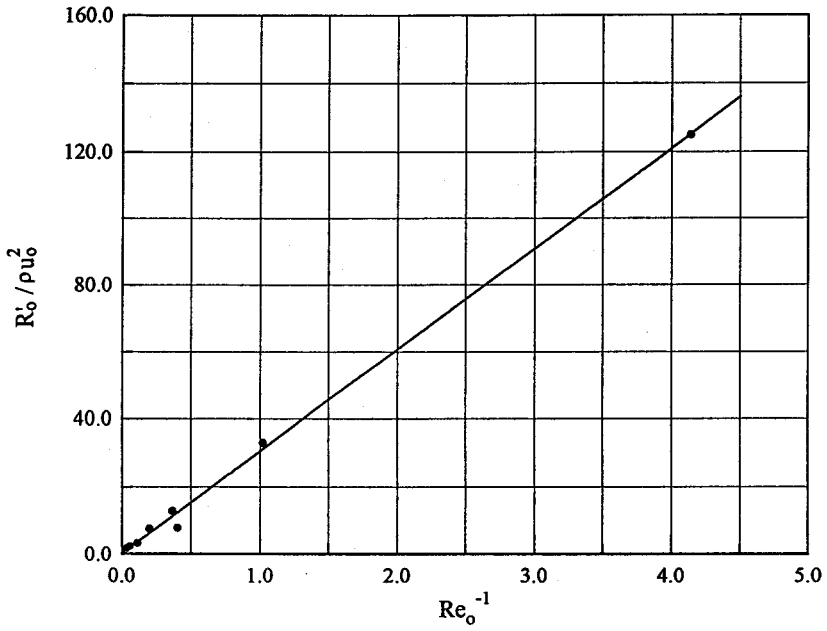


Fig. 6.  $R'_0 / \rho u_0^2$  vs  $Re_0^{-1}$  for cubic particles

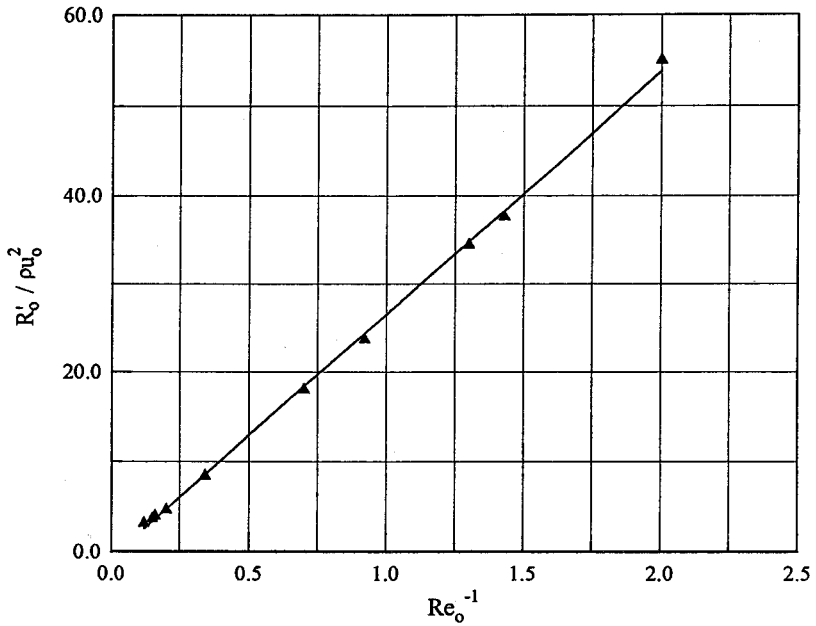
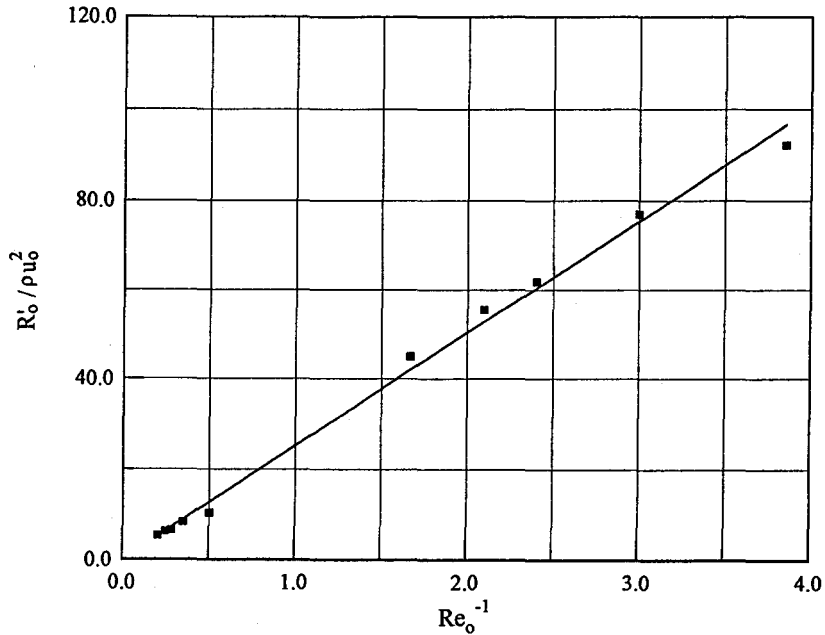


Fig. 7.  $R'_0 / \rho u_0^2$  vs  $Re_0^{-1}$  for rectangular particles

### Drag on Non-Spherical Particles in Non-Newtonian Fluids



**Fig. 8.**  $R'_o / \rho u_o^2$  vs  $Re_o^{-1}$  for cylindrical particles

**Table 3.** Equations Obtained for the Tested Non-Spherical Particles

Particle	Equation	Reynolds Number Range	Coefficient of Correlation
Cubic	$R'_o / \rho u_o^2 = 30.15 Re_o^{-1} + 0.51$	0.25 - 27	0.998
Rectangular	$R'_o / \rho u_o^2 = 27.31 Re_o^{-1} - 0.596$	0.5 - 6	0.999
Cylindrical	$R'_o / \rho u_o^2 = 25.1 Re_o^{-1} + 0.257$	0.25 - 5	0.995

Figures 9, 10 and 11 show the plot  $u_o$  vs  $D_s^2$  (where  $D_s$  is the spherical diameter of the particle and is equal to the diameter of a sphere, whose volume is equal to the volume of the tested non-spherical particle) for the three types of non-spherical particles in glycerol and STP-Oil mixture. All these plots verify the relation obtained by Pettyjohn and Christiansen for non-spherical particles (7) falling at terminal falling velocity. This relation is valid for Reynolds number  $< 0.05$  and is in the following form:

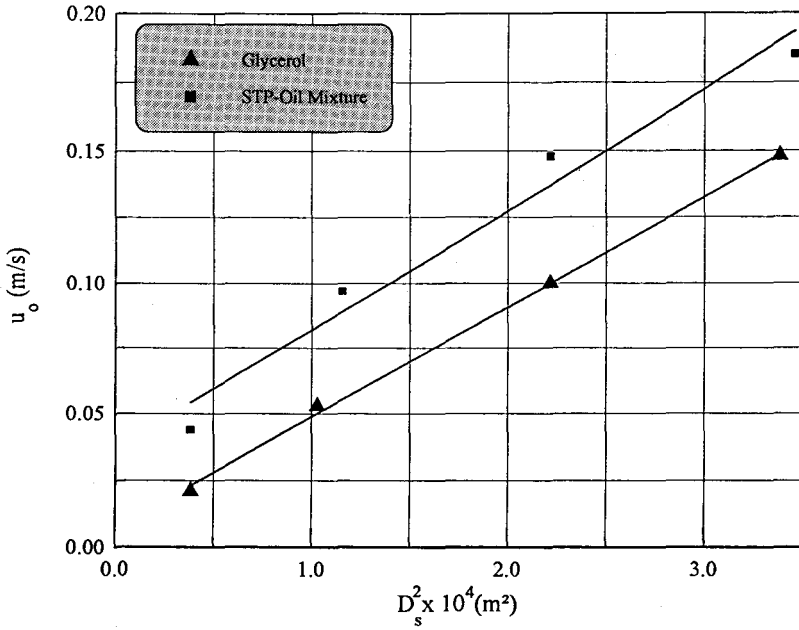


Fig. 9. Terminal falling velocity vs. spherical diameter for cubic particles

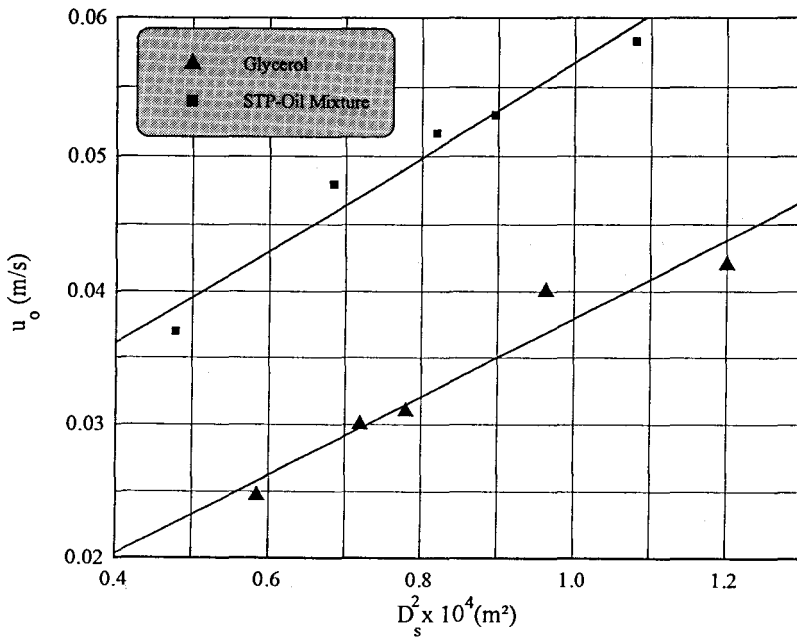


Fig. 10. Terminal falling velocity vs. spherical diameter for rectangular particles

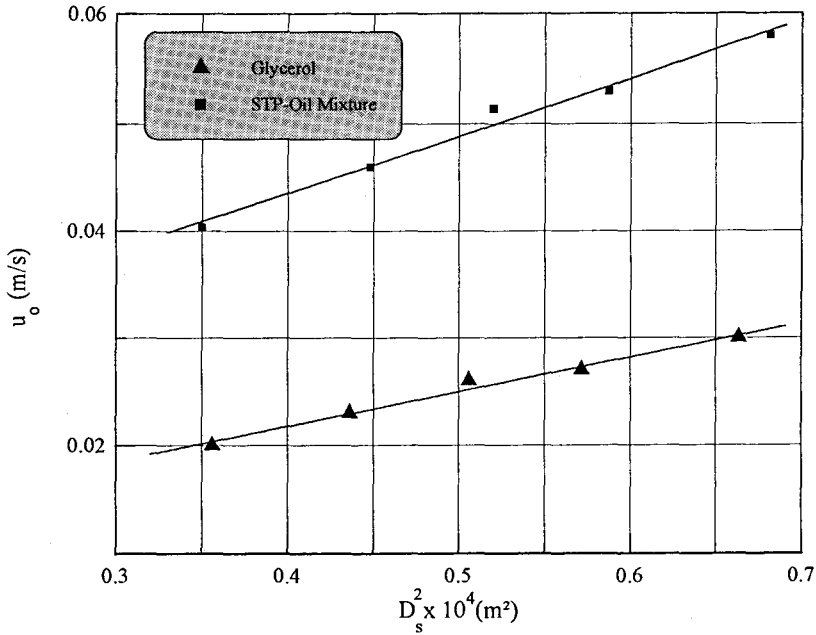


Fig. 11. Terminal falling velocity vs. spherical diameter for cylindrical particles

$$u_o = K_1 \frac{gD_s^2(\rho_p - \rho)}{18\mu}$$

This equation can be written for one fluid and the same material of the particle in the form:  $u_o = K_2 D_s^2$

The different values of  $K_2$  are listed in table 4. From this table it can be noticed that higher values of  $(u_o)$  are obtained for non-spherical particles on falling in glycerol. The reason for that is the use of heavier particles (made of aluminum) in case of glycerol since plastic particles were not able to penetrate the glycerol when put on its surface and stayed floating on the surface. For STP - Oil mixture cylindrical particles would acquire the highest terminal falling velocity as compared to cubic or rectangular particles of the same volume. But for glycerol cubic particles will be the fastest to settle (under conditions of free settling).

Table 4. Different Values of  $K_2$  for the Tested Non-Spherical Particles

Fluid	Values of $K_2$		
	Cubic	Rectangular	Cylindrical
STP-Oil Mixture	0.197	0.150	0.226
Glycerol	0.342	0.234	0.278

Figure 12 shows a plot of  $K_2$  vs  $\log \Psi$  (where  $\Psi$  is the sphericity of the non-spherical particle and is equal to the surface area of a sphere having the same volume as the non-spherical particle divided by the surface area of the non-spherical particle) for STP-Oil mixture. This again agrees with the equation obtained previously by Pettyjohn and Christiansen (7) and the equation obtained in our case is as follows:

$K_2 = 0.504 \log \Psi + 0.2485$  (Coefficient of correlation = 0.999, Reynolds number 2.05 - 26.77).

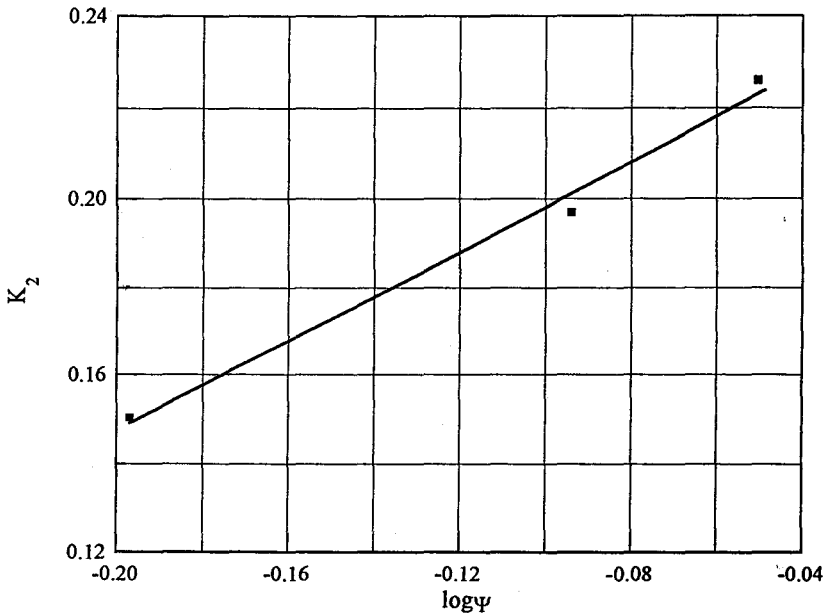


Fig. 12.  $K_2$  vs.  $\log \Psi$  for the tested non-spherical particles in case of STP-Oil mixture



This equation can be rewritten in the form:

$$K_2 = 0.504 \log (\Psi/0.564)$$

The variation in the value of both constants of this equation as compared to that of the equation obtained by Pettyjohn & Christiansen is mainly due to the difference in defining both  $K_1$  and  $K_2$ .

## CONCLUSIONS

- 1- The drag coefficient for three non-spherical particles (cubes, rectangles and cylinders) of different dimension ratios was determined while falling in two non-Newtonian fluids.
- 2- For the three different shapes of the non-spherical particles tested, glycerol (the more viscous non-Newtonian fluids) gave a sharp change in the value of the drag coefficient as compared to STP-Oil mixture (the less viscous non-Newtonian fluid).
- 3- The value of the drag coefficient decreased drastically for cubes as a result of increasing their dimensions; while there was slight decrease in the value for cylinders.
- 4- New mathematical correlations between  $R_o' / \rho u_o^2$  and the modified Reynolds number were obtained for the three non-spherical particles tested (for a Reynolds number range 0.25 - 27).
- 5- Previously published mathematical correlations between  $u_o$  and  $D^2$ ; and  $K^2$  (the coefficient of the previous relation) and log sphericity were verified for the three non-spherical particles tested.

## REFERENCES

1. Pettyjohn, E.S. and Christiansen, E.B., 1948. Chem. Eng. Progress, Vol. 44, No. 2, p.157.
2. Christiansen, E.B. and Barker, D.H., 1965. AIChE Journal, Vol. 11 No. 1, p.145.

3. **Isaacs, J.L. and Thodos, G., 1967 (June).** The Canadian J. of Chem. Eng., Vol. 45, p.150.
4. **Saito, F., Kamiwano, M. and Aoki, R., 1984.** Particulate Science and Technology, Vol. 2, p. 247.
5. **McCabe, W.L., Smith, J.C. and Harriot, P., 1985.** Unit Operations of Chemical Engineering, 4th Edition, McGraw-Hill.
6. **Coulson, J.M., Richardson, J.R.; Backhurst, J.R.; and Harker, J.H., 1991.** Chemical engineering, Vol. 2, 4th Edition, Pergamon Press.
7. **Perry, R.H., Green, D.W.; and Maloney, J.O., 1984.** Perry's Chemical Engineers Hand Book, 6th. Edition, McGraw-Hill.